

Imaging temperature-dependent field emission from carbon nanotube films: Single versus multiwalled

Cite as: Appl. Phys. Lett. **86**, 063109 (2005); <https://doi.org/10.1063/1.1850616>

Submitted: 06 August 2004 • Accepted: 15 November 2004 • Published Online: 02 February 2005

S. Gupta, Y. Y. Wang, J. M. Garguilo, et al.



View Online



Export Citation

ARTICLES YOU MAY BE INTERESTED IN

[Field emission behavior of carbon nanotube field emitters after high temperature thermal annealing](#)

AIP Advances **4**, 077110 (2014); <https://doi.org/10.1063/1.4889896>

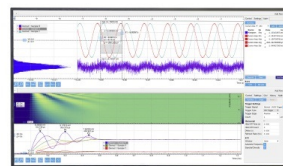
[Electron emission theory and its application: Fowler–Nordheim equation and beyond](#)
Journal of Vacuum Science & Technology B: Microelectronics and Nanometer Structures Processing, Measurement, and Phenomena **21**, 1528 (2003); <https://doi.org/10.1116/1.1573664>

[High-performance field emission device utilizing vertically aligned carbon nanotubes-based pillar architectures](#)

AIP Advances **8**, 015117 (2018); <https://doi.org/10.1063/1.5004769>

Challenge us.

What are your needs for periodic signal detection?



Zurich
Instruments



Imaging temperature-dependent field emission from carbon nanotube films: Single versus multiwalled

S. Gupta,^{a)} Y. Y. Wang, J. M. Garguilo, and R. J. Nemanich

Department of Physics, North Carolina State University, Raleigh, North Carolina 27695-8202

(Received 6 August 2004; accepted 15 November 2004; published online 2 February 2005)

Field emission properties of vertically aligned single- and multiwalled carbon nanotube films at temperatures up to 1000 °C are investigated by electron emission microscopy, enabling real-time imaging of electron emission to provide information on emission site density, the temporal variation of the emission intensity, and insight into the role of adsorbates. The nanotube films showed an emission site density of $10^4 \sim 10^5/\text{cm}^2$, which is compared to the areal density (from $10^{12} \sim 10^{13}/\text{cm}^2$ to $10^8 \sim 10^9/\text{cm}^2$). At ambient temperature, the emission indicated temporal fluctuation ($\sim 6\% - 8\%$) in emission current with minimal changes in the emission pattern. At elevated temperatures, the emission site exhibited an increase in emission site intensity. From the experimental observations, it is proposed that the chemisorbed molecules tend to desorb presumably at high applied electric fields (*field-induced*) in combination with thermal effects (*thermal-induced*) and provide a contrasting comparison between semiconducting (single-walled) and metallic (multiwalled) nanotubes. © 2005 American Institute of Physics. [DOI: 10.1063/1.1850616]

Field emission properties from single- and multiwalled carbon nanotubes (SWNTs and MWNTs) in various forms (individual, mat, and vertically aligned) have been studied by several groups using traditional emission current—applied voltage (*I-V*) characterization and field emission energy distribution.^{1,2} In this context, it is desirable to be able to spatially characterize the origin of the emission of electrons. Field emission is a surface-sensitive phenomenon and, to date, most of the field emission measurements have been performed at room temperature.³ However, temperature-dependent field electron emission microscopy (T-FEEM) can detect changes in the electron emission characteristics, which could provide additional insight on the structure and surface of the nanotubes investigated. Moreover, high-temperature thermionic electron emission from carbon nanotubes (CNTs) has been carried out keeping in view the potential for development of direct thermal-to-electrical power conversion applications.⁴ In this letter, we investigate the intrinsic stability of electron field emission from vertically aligned SWNTs and MWNTs as a function of temperature to elucidate the role of chemisorbed molecules and to determine the thermionic component of the emission.

Films of nanotube emitters for field emission microscopy were prepared following the method described previously.^{5,6} Films of vertically aligned MWNTs and SWNTs were synthesized using microwave plasma-enhanced chemical vapor deposition employing acetylene and ammonia gas mixtures in a 1:4 ratio at relatively high deposition temperatures (~ 900 °C) using an iron (Fe) layer of thickness from 0.5 to 80 nm as catalyst on (SiO_2/Si) substrates. Depending upon the Fe layer thickness, the deposition process resulted in the formation of SWNTs and MWNTs. The SiO_2 layer (~ 180 nm) was used as a diffusion barrier preventing reaction between Si and Fe and the consequent silicide formation. A section of a Si wafer was placed on top of

the catalyst covered growth substrate, and the growth proceeded under the shielded region of the surface. As-deposited CNT samples were characterized using scanning electron microscopy (SEM). Cross-sectional SEM images (top left, Fig. 1) for the as-grown films reveal an apparent difference in surface morphology. In the case of SWNTs, the nanotubes are vertically aligned to the substrate, their distribution is fairly uniform with a height of $\sim 7\text{--}8$ μm , and they appear to be carpet-like.^{5,6}

The FEEM measurements were performed using an UHV-photoelectron emission microscope (Elmitech PEEM III) with a base pressure of less than 3×10^{-10} Torr. The system has sample heating which was used to degas the sample surface at 150 °C and to obtain T-FEEM measurements up to 1000 °C. The field of view was varied between 150 and 2 μm with a resolution of ≤ 15 nm at the highest magnification. For all of the imaging measurements, a voltage of 20 kV is applied between the anode and the sample surface, which is positioned with a nominal separation of 3–4 mm, resulting in an applied field of ~ 5 V/ μm . The electron emission current from the sample surface can be monitored and recorded to obtain the *I-V* dependence. In the process of imaging, the electrons emitted from the sample surface pass through a perforated anode and are imaged using electron optics. The focused electrons are intensified with a microchannel plate (MCP) and imaged with a fluorescent screen. A CCD camera is used for image capturing. The gain of the system is dependent upon the voltage on the image intensifier. In the FEEM measurements the emission was due to only the high applied field, unlike the PEEM measurements, where a 100 W high-pressure mercury short-arc lamp, which provides multiline UV emission with a high-energy cutoff at ~ 5.1 eV, is used to photoexcite the electron emission.⁷

In addition to room temperature measurements, the electron emission imaging was also carried out at elevated temperatures. To quantify the variation in emission site intensity (equivalent to emission site brightness) at ambient and elevated temperatures, we clipped a 270×270 pixel region (equivalent to a 50×50 μm^2 box) from each 150 μm field

^{a)} Author to whom correspondence should be addressed; electronic mail: sxg535f@smsu.edu; present address: Department of Physics, Astronomy, and Materials Science, Southwest Missouri State University, Springfield, MO 65804-0027.

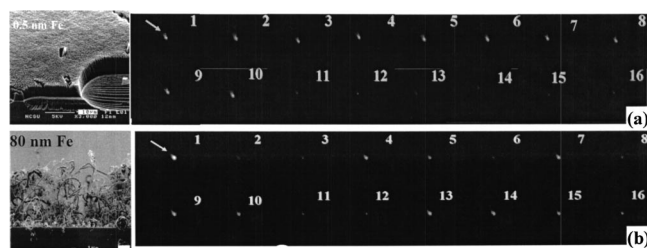


FIG. 1. Shown are the snapshots of field emission imaging demonstrating the emission site intensity variation with time at room temperature for (a) SWNT and (b) MWNT films taken at a $150\ \mu\text{m}$ field of view with 1.15 and 0.85 kV MCP voltage, respectively. Corresponding cross-sectional SEM images are also provided.

of view image (810×810 pixels) and used the image histograms to compute the integrated brightness. This was performed using the DVC View software available with our CCD camera.

To determine the temporal fluctuation, we measured the emission site intensity variation at constant voltage as a function of time at a background pressure of $\sim 10^{-9}$ Torr at ambient temperature for both nanotube surfaces. Figure 1 displays snapshot images of the emission site for the SWNT and MWNT samples. The images are taken successively at a rate of 1/s starting at 0 and ending after at 15 s, resulting in a total of 16 frames. The field emission images were obtained at a $150\ \mu\text{m}$ field of view and at different MCP voltages (1.25 kV for the SWNT and 0.85 kV for the MWNT). Qualitatively speaking, since MWNTs required relatively lower channel plate voltage while monitoring a particular emission site, it implies that the emission from MWNT films was relatively more intense, albeit this may not be valid throughout the sample. In order to establish this point and to draw a concrete conclusion, several more samples of each type of nanotube need to be examined with the goal of comparing emission site intensity.

Qualitatively, these frames [Figs. 1(a) and 1(b)] clearly show temporal fluctuation in emission current of the monitored emission site at ambient temperature under continuous (dc) operation at a background vacuum level of 3×10^{-9} Torr. However, by computing the integrated brightness (not shown) for each frame for both data sets, we find that the short-term fluctuations (or drifts) are on the order of 6%–8% (SW) to 10%–14% (MW). However, for the SWNT film we observe a substantial decrease in the emission site intensity [see Fig. 1(a), frame 10 onwards], unlike the

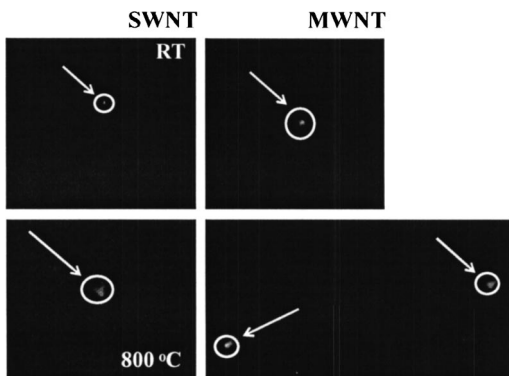


FIG. 2. Temperature dependent field emission imaging for (a) SWNT and (b) MWNT films exhibiting that more emission sites appeared for MWNT at elevated temperature of $800\ ^\circ\text{C}$. The emission site is encircled.

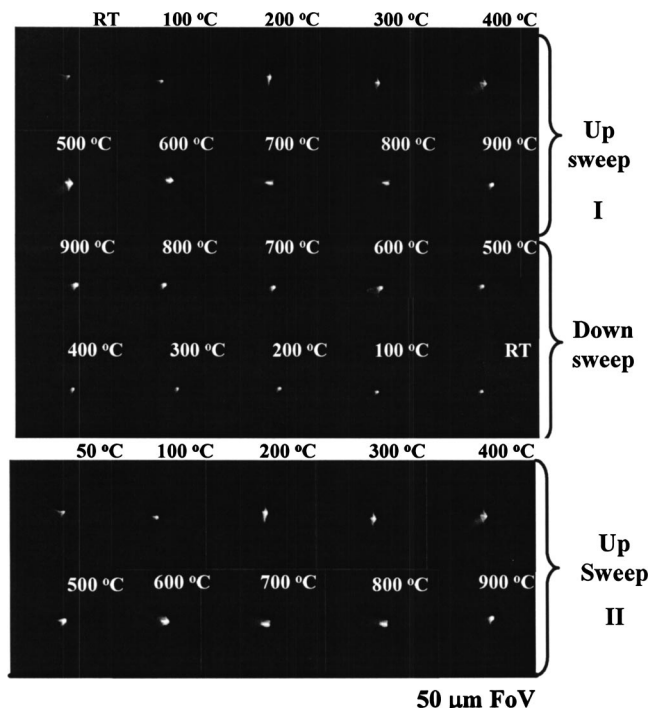


FIG. 3. Temperature-dependent field-emission imaging for a representative MWNT film for warming up and cooling down cycle (represented as cycle I) and warming up again (represented as cycle II). The latter exhibits the thermionic component along with field emission.

MWNT film, which were usually rapidly fluctuating rapidly [Fig. 1(b)]. It is probable that thin tubes (or SWNTs) were gradually destroyed in the high applied fields and/or ion bombardment (which may occur by either gas phase electron ionization or by ion desorption from the anode, both induced by the emitted electrons). These results are similar to those found by Bonard *et al.*,⁸ where they carried out transmission electron microscopy investigations and found that SWNT structure is sensitive to ion bombardment while the MWNT remain relatively less affected.

The FEEM images show distinct emission sites separated by an average of $\sim 150\ \mu\text{m}$, indicating an emission site density of $10^4/\text{cm}^2$, which is much lower than the CNT areal densities of $10^{12} \sim 10^{13}/\text{cm}^2$ and $10^8 \sim 10^9/\text{cm}^2$ for the SW and MW nanotube surfaces (deduced from cross-sectional SEM). We have previously noted that the emission from moderate density nanotube films is relatively more efficient.⁹ Conversely, high-density films such as the SWNT films show reduced emission properties, which may be attributed to screening effects from the densely packed neighboring tubes.¹⁰ The excellent field emission properties of the MWNTs may be due to their invariable metallic character in contrast to SWNTs, which can be both semiconducting and metallic as governed by the chirality of each NT.

Field emission microscopy measurements were carried out as a function of temperature (T-FEEM) to investigate the emission site density and intensity variation. An example of the former is displayed in Fig. 2 and the latter in Fig. 3. From Fig. 2, it appears that besides the increase in the emission site intensity as the temperature is increased, we do observe detectable emission from new sites for the MWNT film.

To further investigate the temperature effect and confirm the role of adsorbates on the field emission and thermionic component, the field emission imaging was measured during two warming up cycles (I and II). The emission intensity

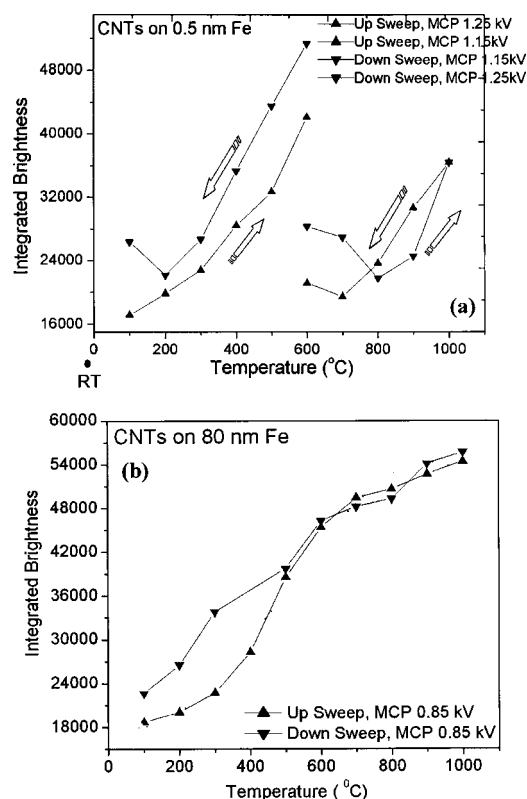


FIG. 4. Variation of integrated brightness with temperature (both up and down sweep) for (a) SWNT and (b) MWNT films. The dotted line is used to guide eye.

from an individual site at various temperatures from RT to 900 °C (cycle I) is shown in Fig. 3 as a representative example for the MWNT films. However, similar results were found for SWNTs, and qualitatively both kinds of films showed increased emission intensity as the temperature is increased (cycle I). In cycle II, after the cleaning or removal of adsorbates, the increase in intensity is attributed to thermionic emission and thermionic field emission.

In Fig. 4, the emission site intensity is plotted as a function of temperature for up and down sweeps (cycle I). These intensities were obtained from clipped $50 \times 50 \mu\text{m}^2$ regions, as described earlier. To avoid saturation, the images were measured at three different channel plate voltages (1.25, 1.15, and 0.85 kV). With increased temperatures the emission intensity of each site increased, and in the case of SWNT, it was necessary to decrease the intensifier voltage from 1.25 to 1.15 kV [see Fig. 4(a), up and down sweep]. We also noticed an increase in background pressure, (from 1×10^{-9} to 1×10^{-8} Torr) which may be attributed to field-induced desorption of the chemisorbed molecules and the resulting change or increase in the emission current intensity. We termed this process as “self-cleaning,” where the adsorbates are partially depleted and the nanotube surface is brought to a new steady state. Additionally, it appears that MWNTs are more sensitive to environment [see Fig. 1(b)] than SWNT surfaces at comparable chamber pressure and emission current. The increase in pressure from 10^{-9} to sub- 10^{-7} Torr with increasing temperature is large enough to justify the presence of adsorbates in a time scale of several minutes, but note that we have not yet identified the species.

As suggested in Ref. 11, we have identified three emission states using field emission microscopy: (i) adsorbate-enhanced (RT), (ii) partially clean nanotubes (cycle I), and

(iii) clean nanotube (cycle II). We note that the transition between the adsorbate-enhanced emission (cycle I; partially cleaned) and the clean nanotubes (cycle II) emission may be achieved due to field-induced desorption in combination with the elevated temperatures (i.e., thermal-induced) and current saturation effect (~ 900 °C for SWNTs and ~ 700 °C for MWNTs). When the temperature exceeds the desorption temperature of the adsorbates, the accompanying enhanced tunneling states are removed, and the field emission is reduced. Under nonideal conditions, the adsorbates may return to the emitting surface when the applied field and temperature is reduced, resulting in a reversible integrated brightness versus temperature characteristics with a slight hysteresis (Fig. 4, down sweep).

In summary, T-FEEM has emerged as an important technique to characterize the (a) temporal stability, (b) temperature dependence, (c) role of adsorbates in affecting the field emission properties, and (d) whether or not there is a thermionic contribution to the field emission from SWNTs and MWNTs. It was found that SWNTs are relatively less sensitive to operating environments than MWNTs, which we attribute to greater resistance to ion damage and effects due to the applied field. At elevated temperatures, an increase in emission sites intensity was found and in second cycle the thermionic component is apparent. The results of the temperature dependence of the field emission suggest that emission from MWNTs seems to be relatively enhanced over that from SWNTs. An important question for future research will be to determine the spatial dependence of field emission, to evaluate thermionic and tunneling components of the emission separately, and to quantify the effect of adsorbates on the electronic properties of nanotube surfaces.

We gratefully acknowledge the Duke University Free Electron Laser Laboratory where all of the field electron emission microscopy experiments were performed. This research work was financially supported in parts by the ONR MURI on Thermionic Energy Conversion and the ANL DOE Center Grants.

- ¹W. B. Choi, D. S. Chung, J. H. Kang, H. Y. Kim, Y. W. Jin, I. T. Han, Y. H. Lee, J. E. Jung, N. S. Lee, G. S. Park, and J. M. Kim, *Appl. Phys. Lett.* **75**, 3129 (1999).
- ²O. Gröning, O. M. Kuttel, Ch. Emmenegger, P. Gröning, and L. Schlappbach, *J. Vac. Sci. Technol. B* **18**, 665 (2000).
- ³F. A. M. Kock, J. M. Garguillo, R. J. Nemanich, S. Gupta, B. R. Weiner, and G. Morell, *Diamond Relat. Mater.* **12**, 474 (2003).
- ⁴S. H. Shih, T. S. Fisher, D. G. Walker, A. M. Strauss, W. P. Kang, and J. L. Davidson, *J. Vac. Sci. Technol. B* **21**, 587 (2003).
- ⁵Y. Y. Wang, F. A. M. Kock, J. M. Garguillo, and R. J. Nemanich, *Diamond Relat. Mater.* **13**, 457 (2004).
- ⁶Y. Y. Wang, S. Gupta, and R. J. Nemanich, *Appl. Phys. Lett.* **85**, 2601 (2004).
- ⁷R. J. Nemanich, S. L. English, J. D. Hartman, A. T. Sowers, B. L. Ward, H. Ade, and R. F. Davis, *Appl. Surf. Sci.* **146**, 287 (1999).
- ⁸J.-M. Bonard, N. Weiss, H. Kind, T. Stöckli, L. Forró, K. Kern, and A. Chatelain, *Adv. Mater. (Weinheim, Ger.)* **13**, 184 (2000).
- ⁹Y. Y. Wang, S. Gupta, M. L. Liang, and R. J. Nemanich, *J. Appl. Phys.* (to be published).
- ¹⁰W. A. de Heer, A. Chatelain, and D. Ugarte, *Science* **270**, 1179 (1995); D. S. Chung, W. B. Choi, J. H. Kang, H. Y. Kim, I. T. Han, Y. S. Park, Y. H. Lee, N. S. Lee, J. E. Jung, and J. M. Kim, *J. Vac. Sci. Technol. B* **18**, 1054 (2000).
- ¹¹R. Collazo, R. Schlessler, and Z. Sitar, *Diamond Relat. Mater.* **11**, 769 (2002); K. A. Dean and B. R. Chalamala, *Appl. Phys. Lett.* **76**, 375 (2000).